Global average of air-sea CO2 transfer velocity from QuikSCAT scatterometer wind speeds

Jacqueline Boutin, Yves Quilfen, Liliane Merlivat, Jean-François Piolle

Global average of air-sea CO_2 transfer velocity from QuikSCAT scatterometer wind speeds

J. Boutin,[1] Y. Quilfen,[2] L. Merlivat,[1] and J. F. Piolle[2]

Received 16 February 2007; revised 28 November 2008; accepted 13 January 2009; published 23 April 2009.

[1] The absolute calibration of the relationship between air-sea CO_2 transfer velocity, k, and wind speed, U, has been a topic of debate for some time, because k global average, $\langle k \rangle$, as deduced from Geochemical Ocean Sections Study oceanic ^{14}C inventory has differed from that deduced from experimental k-U relationships. Recently, new oceanic ^{14}C inventories and inversions have lead to a lower $\langle k \rangle$. In addition, new measurements performed at sea in high–wind speed conditions have led to new k-U relationship. Meanwhile, quality and sampling of satellite wind speeds has greatly improved. The QuikSCAT scatterometer has provided high-quality wind speeds for more than 7 years. This allows us to estimate the global distributions of k computed using k-U relationships and temperature-dependent Schmidt numbers from 1999 to 2006. Given the difficulty of measuring in situ wind speed very accurately, we performed a sensitivity study of the $\langle k \rangle$ uncertainty which results from QuikSCAT U uncertainties. New QuikSCAT-buoy U comparisons in the northern Atlantic Ocean and in the Southern Ocean confirm the excellent precision of QuikSCAT U (RMS difference of about 1 m s^{-1}), but it is possible that QuikSCAT overestimates wind speeds by 5%, leading to a possible overestimation of k derived with quadratic relationships by 10%. The $\langle k \rangle$ values obtained with two recent experimental k-U relationships are very close, between 15.9 and 17.9 cm h^{-1}, and within the error bar of k average deduced from the new oceanic ^{14}C inventory.

Citation: Boutin, J., Y. Quilfen, L. Merlivat, and J. F. Piolle (2009), Global average of air-sea CO_2 transfer velocity from QuikSCAT scatterometer wind speeds, *J. Geophys. Res.*, *114*, C04007, doi:10.1029/2007JC004168.

1. Introduction

[2] The ocean strongly influences the rate of increase of atmospheric CO_2 linked to CO_2 release into the atmosphere by anthropogenic activities. In fact, since preindustrial times, the ocean has absorbed about one third of the CO_2 released in the atmosphere by fossil fuel burning [*Sabine et al.*, 2004]. It is therefore critical for the study of climate that the spatial and temporal distributions of air-sea CO_2 flux be described quantitatively.

[3] Locally, air-sea CO_2 flux, F, can be estimated from surface ocean measurements, using a bulk parameterization:

$$F = k\ S\ \Delta pCO_2, \quad (1)$$

where k is the gas transfer velocity, S is the gas solubility, ΔpCO_2 is the gradient between atmospheric CO_2 partial pressure and surface ocean CO_2 partial pressure, pCO_2. Hence regional estimates of the air-sea gas flux can be deduced from the integration in space and time of F. The main difficulty in these estimates is linked to our incomplete knowledge of (1) pCO_2 variability and (2) the absolute calibration of the relationship between k, wind speed, U, and sea surface state. The pCO_2 is highly variable in space and time as it is affected by CO_2 chemistry in seawater (primarily controlled by sea surface temperature (SST)), by ocean physics (advection and diffusion processes), by biological processes and by air-sea exchange. Ocean physics and biological processes are difficult to model, and there exists no simple relationship between pCO_2 and parameters monitored on a global scale. Therefore, current estimates of large-scale air-sea CO_2 flux from bulk parameterizations use either the monthly climatology of pCO_2 derived on a global scale from the extrapolation of ship measurements [*Takahashi et al.*, 2002], or empirical relationships established on a regional scale between pCO_2 and satellite-derived parameters (such as SST, SST anomalies and chlorophyll). The latter methodology provides an alternative way to study spatial and seasonal to interannual variability (e.g., in the equatorial Pacific [*Boutin et al.*, 1999a; *Etcheto et al.*, 1999; *Feely et al.*, 2002] and in the Southern Ocean [*Rangama et al.*, 2005], in the Chile upwelling [*Lefèvre et al.*, 2002]).

[4] Concerning k, there has been a great deal about the calibration of k-U relationships and the magnitude of its global average. Until recently, the value deduced from global satellite wind speed using experimental k-U relation-

[1] Laboratoire d'Océanographie et du Climat, UMR7159, UPMC, Expérimentation et Approches Numériques, Institut Pierre Simon Laplace, CNRS, Paris, France.
[2] Laboratoire d'Océanographie Spatiale, IFREMER, Brest, France.

0148-0227/09/2007JC004168

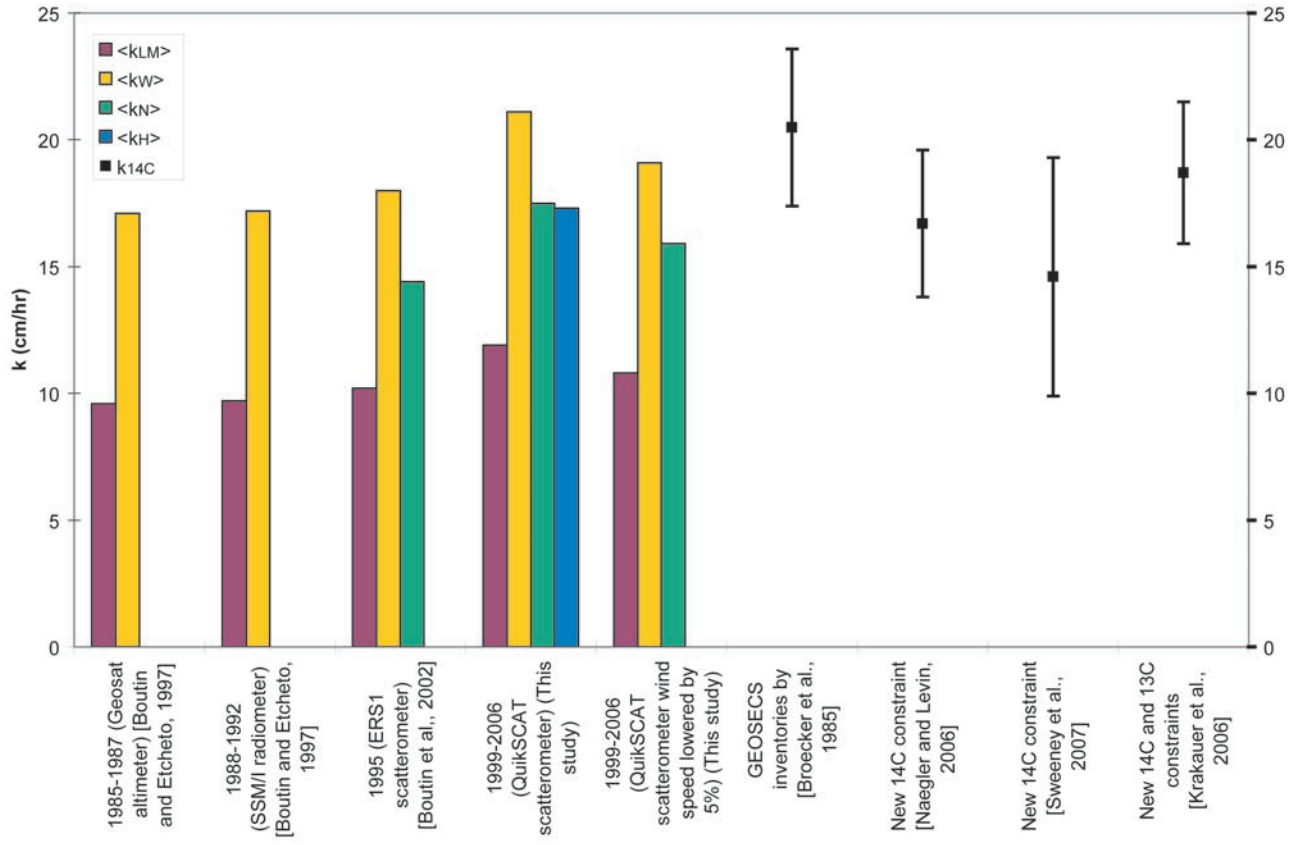

Figure 1. Global averages of k (in cm h^{-1}) deduced from long time series of satellite wind speeds and k-U relationships (bar charts) (maroon bars indicate k_{LM}, yellow bars indicate k_W, green bars indicate k_N, and blue bars indicate k_H) and deduced from ^{14}C global inventories (black squares) (errors are the ones reported in the original papers). The GEOSECS inventory is the *Wanninkhof* [1992] original value at 20°C converted to in situ SST; the *Naegler and Levin* [2006] estimate is deduced from NCEP, European Centre for Medium-Range Weather Forecasts, Special Sensor Microwave Imager (SSMI), QuikSCAT, and ERS2 wind speeds and Ocean Parallelise Ocean General Circulation model; the *Sweeney et al.* [2007] estimate is deduced from NCEP wind speeds and three versions of the Geophysical Fluid Dynamics Laboratory Modular Ocean Model 3 Ocean General Circulation Model; and the original values of *Krakauer et al.* [2006] at 20°C were converted to in situ SST (they assume linear k-U relationship and use SSMI climatological squared wind speed).

ships (Figure 1, left) differed by a factor of 1.2 to 1.8 from the value deduced by *Wanninkhof* [1992] from a k-U relationship calibrated with global Geochemical Ocean Sections Study (GEOSECS) ^{14}C oceanic inventories (Figure 1, right). Recently, new analyses of WOCE measurements revealed that GEOSECS ^{14}C inventories were high-biased [*Peacock*, 2004; *Key et al.*, 2004; *Naegler and Levin*, 2006]. By taking into consideration the new ^{14}C inventories and various inverse models, *Krakauer et al.* [2006], *Naegler et al.* [2006], and *Sweeney et al.* [2007] derive new estimates of global k average that are 9% to 24% lower than the older GEOSECS-based average (Figure 1, right).

[5] Meanwhile, the QuikSCAT scatterometer has provided unprecedented high-quality satellite wind speeds for more than 7 years. Since its launch, in 1999, it has monitored the surface wind speed at 25 km resolution with almost global ocean coverage every day. In addition, validations with in situ wind speeds indicate that the quality of scatterometer wind speeds is better than that of other remotely sensed wind speeds. Since a good knowledge of both the average and the variability of the wind speed is crucial to constraining k average [*Wanninkhof*, 2007; *Wanninkhof et al.*, 2002], we can take advantage of this lengthy time series of high-quality wind speeds to estimate the global average of k, $\langle k \rangle$, over 7 years (1999–2006) using four k-U relationships. The objective of this paper is to compare these with the new ^{14}C-derived k global averages, and to analyze to what extent the differences are compatible with satellite wind speed uncertainty. With respect to previous $\langle k \rangle$ estimates based on remotely sensed wind speeds, we use recent empirical k-U relationships and a longer time series of wind speeds obtained with a single instrument (avoiding differences due to instrument change) which allows us to estimate an interval of uncertainty for $\langle k \rangle$. The latter is based on already published comparisons of QuikSCAT wind speeds with in situ wind speeds and on new QuikSCAT-in situ wind speed comparisons in the northern Atlantic and in the Southern Ocean. They cover a very large range of moderate to strong wind speeds, enabling a validation of wind speed variability and intensity. This is all the more relevant for air-

sea CO_2 flux studies as the Southern Ocean is a region where very few wind validations have been conducted, and where the CO_2 sink is quite large, because of strong wind speeds [*Boutin et al.*, 2002; *Ho et al.*, 2006].

[6] This paper is organized as follows: data and methods are described in section 2, the uncertainty on QuikSCAT wind speeds is estimated in section 3, global averages of k are presented in section 4, and the summary and conclusion are given in section 5.

2. Data and Methods

2.1. Data

2.1.1. Satellite Wind Speeds

[7] Three types of satellite instruments have been used in the past to derive k from satellite wind speeds [e.g., *Boutin and Etcheto*, 1997; *Carr et al.*, 2002]. The advantages and disadvantages of each type of instrument for the determination of k as presented in previous studies [*Boutin and Etcheto*, 1996; *Boutin et al.*, 1999b] are summarized below.

[8] An altimeter (e.g., Geosat, TOPEX-POSEIDON, JASON) measures the radar signal reflected specularly to the instrument by the sea surface. It performs better at low to moderate wind speeds. The altimeter wind speed is derived at about 7 km resolution. The altimeter swath is narrow, about 5 km wide. Hence altimeter k fields are undersampled.

[9] A microwave radiometer (e.g., Special Sensor Microwave Imager, WindSat) measures the radiation emitted by the sea surface at several wavelengths. Since the emissivity is dependent on geophysical parameters (atmospheric water, SST, etc) other than surface wind, flaws in the correction of these effects may lead to regional biases. Its swath is wide (1000–1400 km) and the resolution of individual measurements is typically 25 km.

[10] A scatterometer (e.g., ERS, NSCAT, QuikSCAT) measures the radar signal backscattered to the instrument by the sea surface (Bragg scattering by gravity-capillary waves). It provides very accurate satellite wind speed, in particular because it has very little sensitivity to atmospheric conditions. Although wind speed retrieval from microwave radiometers such as WINDSAT has improved, the scatterometer wind speeds have a better sensitivity at low and moderate wind speeds [*Quilfen et al.*, 2007]. *Freilich and Vanhoff* [2006], comparing satellite with National Data Buoy Center (NDBC) buoy wind speeds, found an RMS difference of 1.2 m s^{-1} between QuikSCAT and NDBC wind speeds and of 1.4 m s^{-1} between WINDSAT and NDBC wind speeds. Scatterometer swaths are wide (500–1600 km) and the resolution of individual measurements varies between 12.5 and 50 km. Over a $1° \times 1°$ area and 10 days, there are approximately 240 independent wind speed measurements at 25 km resolution derived from the QuikSCAT scatterometer, whereas there are about 30 independent wind speed estimates from one altimeter instrument.

[11] In this study, we utilize QuikSCAT wind speeds from September 1999 to August 2006. In order to take the effects of wind speed variability on k into account, we compute k for each high-resolution wind speed. We use the level 2B QuikSCAT wind speeds at 25 km resolution derived at NASA/JPL (http://podaac.jpl.nasa.gov/DATA_PRODUCT/OVW/index.html; nudge product processed with version 2.4 until May 2006; rain flagged wind speeds discarded). A new version of QuikSCAT wind speeds was released in summer 2006. With respect to version 2.4, high wind speeds (over 20 m s^{-1}) have been increased and flagging of rain contamination has been improved. However, the comparison of weekly k fields generated by the two versions for June 2006 shows small differences in large-scale k distributions: the difference is lower than 2% in the global k average and lower than 3% in regional k averages.

2.1.2. In Situ Wind Speed

[12] QuikSCAT wind speeds are compared (1) in the northern Atlantic with wind speeds measured during the Program Ocean Multidisciplinary MEsoscale (POMME) experiment on a meteorological buoy and four carbon interface ocean atmosphere (CARIOCA) drifters and (2) in the Southern Ocean with wind speeds recorded on five CARIOCA drifters. Periods and locations of colocations are summarized in Appendix A. In situ wind speeds are either measured at 2 m height, U2m, or at 4.5 m height, U4.5m. They are adjusted to 10 m height wind speed, U10m, either using a constant drag coefficient, or using the *Liu and Tang* [1996] algorithm which computes the wind speed at 10 m height that would have been observed for the same friction velocity under a neutrally stable atmosphere.

[13] CARIOCA drifters are autonomous instruments primarily designed to measure parameters at the air-sea interface related to air-sea CO_2 flux [*Bakker et al.*, 2001; *Hood and Merlivat*, 2001; *Merlivat and Brault*, 1995]. They are designed for a period of autonomy of 1 year. In addition to sea surface CO_2 partial pressure and fluorescence, they measure U2m, and (since 2004) air temperature at 2 m height above the sea surface, the atmospheric surface pressure and the sea surface temperature at 2 m depth. CARIOCA drifters follow sea surface currents at about 15 m depth by using a "holey sock" drogue. Hence they measure the wind speed relative to the sea surface drift (always less than 1 m s^{-1}; averaged over all buoys in the Southern Ocean, the east-west speed of the buoys is 0.2 m s^{-1}). Scatterometer measurements are primarily sensitive to the surface wind stress and therefore to the wind speed relative to sea surface currents [*Kelly et al.*, 2001; *Quilfen et al.*, 2001]. Consequently, the use of in situ wind speeds relative to sea surface drift should reduce differences in the comparisons between in situ and satellite wind speeds, avoiding regional biases due to the presence of strong currents. In addition, k is also sensitive to surface wind stress so that wind speed relative to sea surface drift and scatterometer wind speeds are better proxies for k than wind speed in a terrestrial reference frame.

[14] Before 2004, CARIOCA buoys were equipped with cup "Debucourt" anemometers. Debucourt anemometers were tested during the TOSCANE-T campaign [*Queffeulou et al.*, 1988] on moored buoys. After two months, wind speeds measured by the three Debucourt anemometers remained very consistent (mean bias negligible, equal to 0.03 m s^{-1} and the root mean square of the differences equal to 0.18 m s^{-1}). Since 2004, CARIOCA buoys have been equipped with Sonic CV3F anemometers built by the LCJ company (http://www.lcjcapteurs.com). The sensitivity of the LCJ anemometer is 0.2 m s^{-1}.

2.1.2.1. Buoy Wind Speeds in the Northern Atlantic Ocean

[15] The POMME experiment took place in 2000 and 2001 in the northeast Atlantic. Four CARIOCA drifters were

deployed and drifted between 36°N and 46°N and 12°W and 22°W. The POMME meteorological buoy was moored at 20.04°W, 41.6°N and was equipped with a cup anemometer from Vector instruments [*Caniaux et al.*, 2005] which recorded wind speed at 4.5 m height above sea surface, U4.5m.

[16] Both wind speeds are converted to 10 m height wind speed, U10m, assuming a constant drag coefficient, Cd, equal to 1.5×10^{-3}. This corresponds to an adjustment by a multiplicative factor of 1.18 between U2m and U10m and 1.08 between U4.5m and U10m. Tests conducted using the dependence of Cd on U measured during the POMME experiment show that the approximation of a constant Cd does not significantly modify the two fits (mean U10m modified by less than 1%). No correction for air stability was applied because air temperature on CARIOCA buoys was not available before 2004, but an a posteriori correction will be considered in section 0.

2.1.2.2. In Situ Wind Speeds in the Southern Ocean

[17] Between 2001 and mid-2006, nine CARIOCA drifters have been deployed in the Southern Ocean [*Boutin et al.*, 2008]. Unfortunately, some anemometers broke down very rapidly and problems with onboard processing prevented wind speed measured by four of these drifters from being used. Nevertheless, 5 CARIOCA drifters successively recorded wind speeds for 14 months between 40°S and 58°S, providing a unique set of wind speeds in this rough environment (see Appendix A).

[18] For conversion of U2m to neutral wind speeds at 10 m height, before 2004 the atmosphere is assumed to be neutral. After 2004, air-sea temperature differences are taken into account. Two meter height wind speeds are converted to 10 m height neutral wind speeds, taking into account air-sea temperature differences when available, using the *Liu and Tang* [1996] algorithm typically used to validate scatterometer wind speeds with in situ measurements, and assuming a relative humidity of 80%. For a neutral atmosphere, the conversion factor is minimum at 5 m s^{-1} (1.16) and increases at lower and higher wind speeds (1.2 at 15 m s^{-1}).

[19] The influence of atmospheric stability is small at high wind speed. However, in the Southern Ocean the atmosphere is frequently colder than the surface ocean by several degrees so that not correcting for atmospheric stability may lead to a small bias in 10 m neutral wind speed estimates. From 2006 CARIOCA data, we find that the atmosphere stability correction increases the mean CARIOCA 10 m wind speed by 0.15 m s^{-1}.

2.1.3. Sea Surface Temperature

[20] The sea surface temperature, SST, is taken from monthly SST maps derived using a blended analysis between AVHRR (Advanced Very High Resolution Radiometer) and in situ data according to the method described by *Reynolds et al.* [2002]. These maps are available at ftp://podaac.jpl.nasa.gov/pub/sea_surface_temperature/reynolds/oisst/data/oiweek_v2.

2.2. Methods

2.2.1. The k Computation

[21] When dealing with the relationship between k and sea state and gas parameters, experimental k is usually expressed at a constant Schmidt number of 600 (corresponding to the CO_2 Schmidt number in fresh water at a temperature of 20°C [e.g., *Nightingale et al.*, 2000; *Ho et al.*, 2006] or 660 (corresponding to the CO_2 Schmidt number in seawater at a temperature of 20°C [e.g., *Wanninkhof*, 1992]. When studying air-sea CO_2 flux over the ocean it is necessary to take temperature variation into account, since k varies by more than a factor of 2 between 0° and 30°C for CO_2 gas because of variation of the Schmidt number with temperature. This is the reason why, when treating air-sea CO_2 flux using bulk formula (equation (1)), it is more convenient to consider the CO_2 exchange coefficient, K = k S, as temperature variations of k and S almost compensate for each other [*Etcheto and Merlivat*, 1988]. Taking the variation of K as proportional to $((Sc/660)^{-0.5}\ S)$, K varies by less than 10% between 0 and 30°C. In this paper, we derive a global mean value of k, $\langle k \rangle$, from $\langle K \rangle$, the global mean value of K, using a constant ratio between $\langle k \rangle$ and $\langle K \rangle$ defined below. The K fields are derived from high-resolution wind speed data and sea surface temperature maps as described in Appendix B. The temporal and spatial variability of K from 1999 to 2006 is presented in Appendix B.

[22] The following k-U relationships are considered in this paper:

[23] 1. The *Liss and Merlivat* [1986] relationship, which takes into account the physics of the air-sea interface, deduced from wind tunnel measurements, and from lake measurements for normalization. It is divided into three regimes: smooth surface, rough surface, and breaking waves regimes:

$$k_{LM} = 0.17\ U(600/Sc)^{2/3} \quad \text{for} \quad U \leq 3.6\ \text{m s}^{-1} \tag{2a}$$

$$k_{LM} = (2.85\ U - 9.65)(600/Sc)^{0.5} \quad \text{for} \quad 3.6\ \text{m s}^{-1} < U \leq 13\ \text{m s}^{-1} \tag{2b}$$

$$k_{LM} = (5.9\ U - 49.3)(600/Sc)^{0.5} \quad \text{for} \quad U > 13\ \text{m s}^{-1}. \tag{2c}$$

[24] 2. The *Wanninkhof* [1992] quadratic relationship deduced from a quadratic fit to the GEOSECS bomb ^{14}C inventory for short-term wind speed:

$$k_W = 0.31\ U^2(660/Sc)^{0.5}. \tag{3}$$

[25] 3. The *Nightingale et al.* [2000] relationship deduced from dual tracer experiments at sea:

$$k_N = \left(0.222\ U^2 + 0.333\ U\right)(600/Sc)^{0.5}. \tag{4}$$

[26] 4. The *Ho et al.* [2006] relationship recently derived from k measurements performed during the SAGE experiment in the Southern Ocean. It is a quadratic k-U relationship close to the second-order polynomial relationship of *Nightingale et al.* [2000] and 22% lower than that of *Wanninkhof* [1992]. The k corresponding to the *Ho et al.* [2006] relationship ($k_H = 0.266\ U^2\ (600/Sc)^{0.5}$) is deduced from k_W as

$$k_H = 0.818\ k_W. \tag{5}$$

[27] Recently, *Sweeney et al.* [2007] proposed a new relationship based on a new analysis of ^{14}C measurements ($k = 0.27\ U^2\ (660/Sc)^{0.5}$) that are equal to $0.87 \times k_W$.

[28] These k-U relationships, for a Schmidt number of 660 are shown in Appendix B.

[29] A cubic k-U relationship is not considered, as results from the SAGE (SOLAS Air-Sea Gas Exchange) experiment reveal that a quadratic k-U relationship is closer to the measurements than a cubic relationship [*Ho et al.*, 2006], and because differences between quadratic and cubic relationships have already been studied [*Boutin et al.*, 2002].

[30] We compute k from high-resolution wind speed in order to take correctly into account the wind speed variability in the nonlinear k-U relationship. Actually, *Wanninkhof et al.* [2002] show that, on a local scale, the statistical distribution of wind speed frequently differs from a Rayleigh distribution so that relationships between k and "long-term" (averaged) wind speeds calibrated assuming a Rayleigh distribution such as the one proposed by *Wanninkhof* [1992] overestimate k [*Olsen et al.*, 2005].

[31] The global k averages presented in the following sections are deduced from the temporal and spatial integration (area weighted) of K fields. Deriving a global average of k, either from the global average of K or from the global average of k at a Schmidt number of 660, $\langle k_{660} \rangle$, as reported by some authors, is not straightforward because, over the global ocean, wind speed and sea surface temperature are anticorrelated. In order to find conversion factors between $\langle k \rangle$, $\langle K \rangle$ and $\langle k_{660} \rangle$, we compute their ratios over 1 year (2003) as derived from QuikSCAT wind speeds and for a quadratic k-U relationship:

$$\langle K[\text{mol m}^{-2}\ \text{a}^{-1}\ \mu\text{atm}^{-1}] \rangle / \langle k[\text{cm h}^{-1}] \rangle = 3.25 \times 10^{-3}. \quad (6)$$

$$\langle k \rangle / \langle k_{660} \rangle = 0.93. \quad (7)$$

These ratios vary by less than 1% from one year to another ($1\ \text{atm} = 10^5 \times 1.01325\ \text{N m}^{-2}$).

[32] The mean difference between $\langle k \rangle$ and $\langle k_{660} \rangle$ is mainly because the global average of SST is closer to 18°C than to 20°C and because of wind speed−sea surface temperature anticorrelation; it is consistent with the 6% bias found by *Sweeney et al.* [2007] on the calibration of the *Wanninkhof* [1992] k-U relationship which was performed using a constant solubility at 20°C.

2.2.2. Colocation of QuikSCAT With in Situ Wind Speed

[33] Each in situ wind speed is colocated with QuikSCAT measurements taken within a radius of 12.5 km and 30 min. Fits between in situ and QuikSCAT wind speeds are calculated as orthogonal regressions, which makes the implicit assumption that the noise on in situ and QuikSCAT wind speeds is similar. The fit quality is quantified by the 95% confidence interval of the fit slope and by the RMS (root mean square) of QuikSCAT wind speed minus the fit estimate (RMS of (Y-Yfit)).

[34] CARIOCA wind speeds are measured every hour but each measurement is integrated over a very short duration (30 s) in order to save energy. Hence, before comparing QuikSCAT and CARIOCA wind speeds, CARIOCA wind speeds are smoothed with a running average over 3 consecutive measurements weighted by (0.25, 0.5, 0.25) factors. Assuming a rough equivalence between time and space integration that follows the hypothesis of frozen turbulence ($\Delta S = U\ \Delta T$, where ΔS is the spatial extent of the integration, ΔT is the integration duration and U is the wind speed), an integration over 25 km, close to QuikSCAT wind speed resolution, is roughly equivalent to an integration over 2 h at 10 m s^{-1}. This is consistent with a running average over 3 consecutive buoy measurements. This running average decreases the RMS of (Y-Yfit) by about 20% without significant change in the orthogonal fit. Without this running average, the standard deviation of CARIOCA wind speeds is increased by about 4% and estimates of the mean of U squared do not significantly change.

3. QuikSCAT Wind Speed Uncertainty

[35] The validation of satellite wind speed is a tricky task as (1) calibration of in situ wind speed measurements within a few tenths of m s^{-1} is difficult, (2) wind speed is very variable inside a satellite pixel (25 km resolution), and (3) the parameters necessary to compute neutral equivalent wind speed at 10 m height, (wind speed, relative humidity and air temperature at 10 m height, sea surface temperature and currents) are rarely available.

[36] In this section, after recalling recent results for QuikSCAT validation, we present a new set of comparisons between QuikSCAT and in situ wind speeds in the Northern Atlantic at more than 350 km from coasts and in the Southern Ocean at more than 500 km from continental coasts. This is intended to evaluate QuikSCAT wind speed over a large range of moderate to high wind speeds, in regions not frequently sampled by buoys typically used for QuikSCAT validation.

3.1. Previous Studies

[37] Several studies have inferred the quality of QuikSCAT wind speeds from comparison with either buoys, ship or model wind speeds. Comparisons with in situ data [*Bourassa et al.*, 2003; *Ebuchi et al.*, 2002; *Freilich and Vanhoff*, 2006] indicate a root mean square accuracy of QuikSCAT wind speeds between 1 and 1.2 m s^{-1} in conditions without rain. There was no evidence for large systematic biases in QuikSCAT wind speeds. *Ebuchi et al.* [2002] compared QuikSCAT with wind speeds of buoys operated by the National Data Buoy Center (NDBC), Tropical Atmosphere Ocean (TAO), Pilot Research Moored Array in the Tropical Atlantic (PIRATA) project and Japan Meteorological Agency (JMA) in the tropical oceans and in the northern hemisphere,. They found no systematic dependence of buoy-QuikSCAT wind residuals between 5 and 15 m s^{-1} and mean residuals of about -0.5 m s^{-1} for wind speeds greater than 15 m s^{-1} but these latter results have to be taken with caution given the difficulty of measuring high in situ wind speeds. *Freilich and Vanhoff* [2006] found that there were relatively slightly more QuikSCAT wind speeds in the band 10–16 m s^{-1} than National Centers for Environmental Prediction (NCEP) (U.S. National Centers for Environmental Prediction operational numerical weather prediction model) wind speeds when looking at the statistical distributions of colocated wind speeds. It is unlikely that the latter is only due to a larger smoothing of wind

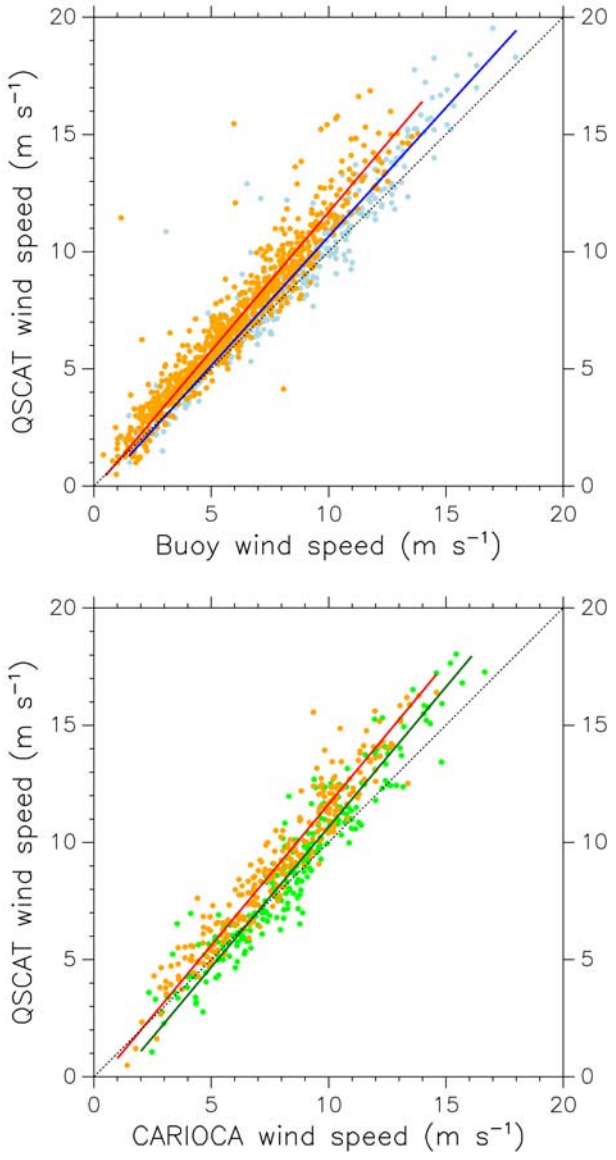

Figure 2. QuikSCAT wind speed versus 10 m in situ wind speed. Statistics of the comparisons are given in Table 1. The 1:1 line is indicated as a dashed line. (top) Comparisons in the northern Atlantic during the POMME experiment with CARIOCA (Debucourt anemometer) (orange points) and meteorological buoy (light blue points) wind speed. Red and blue lines indicate orthogonal regression lines for the CARIOCA-QuikSCAT and meteorological buoy–QuikSCAT comparisons, respectively. (bottom) CARIOCA wind speed in the Southern Ocean. CARIOCA measured with Debucourt anemometer (converted to 10 m height without correction for atmosphere stability) (orange points) and with Sonic anemometer (converted to 10 m height with correction for atmosphere stability) (green points). Red and green lines indicate orthogonal regression lines between QuikSCAT and CARIOCA-Debucourt anemometer wind speeds and between QuikSCAT and CARIOCA–Sonic anemometer wind speeds, respectively.

speed variability by NCEP than by QuikSCAT as *Freilich and Vanhoff* [2006] observed similar differences in the statistical distributions of QuikSCAT wind speeds colocated with NDBC (National Data Buoy Center) buoy wind speeds. These slight differences in wind speed distributions did not affect the average of colocated wind speed because they were compensated by slightly lower QuikSCAT than NCEP wind speeds between 5 and 8 m s^{-1}. The mean QuikSCAT wind speed, $\langle$Uqscat$\rangle$, is 7.23 m s^{-1} and the mean NCEP wind speed, $\langle$Uncep$\rangle$, is 7.22 m s^{-1}. On the other hand, the differences in wind speed distributions affect the standard deviation: the standard deviation of QuikSCAT wind speeds, σqscat, equals 3.04 m s^{-1}, while the standard deviation of NCEP wind speeds, σncep, equals 2.68 m s^{-1}. Assuming that k is proportional to the square of U, we can compute the ratio between the mean of k derived from QuikSCAT wind speeds, $\langle$kqscat$\rangle$ and the mean of k derived from NCEP wind speeds, $\langle$kncep$\rangle$ as:

$$\frac{\langle kqscat\rangle}{\langle kncep\rangle} = \frac{\langle Uqscat\rangle^2 + \sigma qscat^2}{\langle Uncep\rangle^2 + \sigma ncep^2}. \quad (8)$$

[38] We find a 1.04 ratio between $\langle$kqscat$\rangle$ and $\langle$kncep$\rangle$. Over the global ocean, the difference may be even larger as the colocated distributions studied by *Freilich and Vanhoff* [2006] were limited to low and middle latitudes and hence were biased toward low to moderate wind speed. Up to the present date most of the QuikSCAT in situ wind speeds comparisons were based on measurements taken in the equatorial region and in the northern hemisphere.

3.2. Comparison of QuikSCAT With in Situ Wind Speed in the Northern Atlantic

[39] The scatterplot of the comparisons between QuikSCAT and CARIOCA wind speeds is shown on Figure 2 (top) and the statistics are given in Table 1. The scatter of the points is remarkably low, the RMS of QuikSCAT wind speed with respect to the orthogonal fit being always lower than 1.03 m s^{-1}. This illustrates the excellent sensitivity of the scatterometer signal to wind speed.

[40] Buoy 10 m wind speeds are systematically lower than QuikSCAT by 13% for CARIOCA and 4% for the moored buoy (Table 1). The comparison of the two fits indicates that for QuikSCAT wind speeds equal to 10 m s^{-1}, CARIOCA wind speeds are lower than moored buoy wind speeds by about 8%. Both fits have a slope significantly higher than 1.

3.3. Comparison of QuikSCAT With in Situ Wind Speed in the Southern Ocean

[41] The scatterplot of the comparisons between QuikSCAT and CARIOCA wind speeds is shown on Figure 2 (bottom) and the statistics are given in Table 1. The scatter of the points is as low as in the northern Atlantic, about 1 m s^{-1}, confirming the excellent correlation of QuikSCAT wind speeds with in situ wind speeds. The orthogonal fit found between the CARIOCA wind speeds as measured with the Debucourt anemometer and QuikSCAT wind speeds is very similar to that found over the POMME area. Both fits have a slope significantly higher than 1. For the same QuikSCAT wind speed values, Sonic anemometer wind speeds are

Table 1. Statistics of QuikSCAT and in Situ 10 m Neutral Wind Speed Comparisons and Equations of Orthogonal Regression Lines

Region	Anemometer Type	$\langle U_{insitu} \rangle$ (m s^{-1})	$\langle U_{qscat} \rangle$ (m s^{-1})	Equation of Orthogonal Fit	95% Confidence Limit on Slope	RMS (Y-Yfit) (m s^{-1})	N
North Atlantic	Debucourt cup[a]	5.99	6.93	$U_{qscat} = 1.18\ U_{in\_situ} - 0.16$	1.16–1.21	0.95	897
North Atlantic	Vector cup[a]	8.33	8.80	$U_{qscat} = 1.10\ U_{in\_situ} - 0.38$	1.07–1.14	1.03	348
Southern Ocean	Debucourt cup[a]	7.87	9.07	$U_{qscat} = 1.20\ U_{in\_situ} - 0.40$	1.16–1.25	0.91	261
Southern Ocean	Sonic	8.60	8.99	$U_{qscat} = 1.19\ U_{in\_situ} - 1.28$	1.14–1.24	1.02	238

[a]The 2 m height in situ wind speeds converted to 10 m height wind speeds assuming stable conditions.

about 1 m s^{-1} higher than Debucourt anemometer wind speeds.

3.4. Discussion

3.4.1. In Situ Wind Speed

[42] The fits between QuikSCAT and CARIOCA wind speeds measured with the Debucourt anemometer in the northern Atlantic and in the Southern Ocean are very similar, indicating a similar bias of QuikSCAT wind speeds in the Southern Ocean and in the northern Atlantic Ocean even though sea state conditions may be different. In both cases, the ratio between QuikSCAT and CARIOCA-Debucourt wind speeds computed from mean values reported in Table 1 is 1.16. However, the fits between QuikSCAT and meteorological buoy wind speeds in the northern Atlantic Ocean and between QuikSCAT and CARIOCA Sonic wind speeds in the Southern Ocean are both lower (by 0.8 m s^{-1} for a QuikSCAT wind speed of 10 m s^{-1}) than the values given by the fits between QuikSCAT and CARIOCA-Debucourt anemometer wind speeds. Hence an underestimation of 8% for CARIOCA-Debucourt wind speeds cannot be excluded. Once this effect is accounted for, and once a correction of 0.15 m s^{-1} for neutral atmosphere assumption (see section 0) is added to our comparisons, CARIOCA wind speeds in the northern Atlantic Ocean and in the Southern Ocean still remain lower than QuikSCAT wind speeds by about 5% (Table 2). In addition the variability of in situ wind speed is found to be lower than the variability of QuikSCAT wind speeds. Using an equation similar to equation (8), we find ratios of 1.08 to 1.12 between mean k deduced from QuikSCAT wind speeds and from in situ wind speeds (Table 2, last column).

[43] Since this difference is estimated from 9 buoys of 3 different types, in several oceans and at various seasons, it is unlikely that it is due to a flaw in anemometer calibration. One uncertainty could result from the model that we use to convert 2 m height wind speed to 10 m height neutral wind speed. The wind stress drag coefficients Cd, deduced from the *Liu and Tang* [1996] algorithm, vary between 1.1×10^{-3} at 5 m s^{-1} and 1.7×10^{-3} at 15 m s^{-1}. These values agree well with the parameterization of Cd deduced from measurements performed in the northern Atlantic during the POMME experiment [*Caniaux et al.*, 2005]. In order to increase the conversion factor between U2m and U10m by 5%, Cd at 15 m s^{-1} should reach 2.5×10^{-3}. Although large uncertainties remain in Cd because it depends on parameters other than wind speeds, this value appears larger than Cd estimated using wave-age or wave-steepness formula in wind sea conditions at high wind speed [*Drennan et al.*, 2005, Figure 9a] showing Cd close to 2×10^{-3} at 15 m s^{-1} in wind sea conditions) and over the global ocean by *Kara et al.* [2007].

3.4.2. QuikSCAT Wind Speed Uncertainty

[44] Once possible biases in in situ wind speeds have been corrected (about 0.7 m s^{-1} at 14 m s^{-1}), the buoy-QuikSCAT wind speed differences we observe are slightly higher than those shown by *Ebuchi et al.* [2002]. Like *Freilich and Vanhoff* [2006], we find greater variability in QuikSCAT wind speed than in in situ wind speed; however the ratio between averages of U squared is slightly higher in our study (Table 2, last column) than are those deduced from their study (see section 3.1). Measuring in situ neutral wind speed with an absolute accuracy better than 0.5 m s^{-1} is very challenging and we cannot definitely assert that our in situ wind speeds are free of biases. On the other hand, validation of QuikSCAT wind speed is also very challenging because few high wind speeds are measured in situ onboard NDBC and tropical buoys, while Ku band scatterometer measurements saturate at high wind speed and rain disturbs wind speed retrieval. In this paper we have presented a new set of in situ measurements allowing the validation of QuikSCAT wind speeds in regions that have never been validated from buoy observations in the past (Southern Ocean) and where high wind speeds occur.

[45] All these studies agree on the fact that scatterometer QuikSCAT wind speeds are of extremely good quality, but that, in the worst case scenario, they could suffer from an overestimation by less than 5%. Hence, in the following analyses, we assume that QuikSCAT wind speed can be taken as the reference wind speed, but we have also performed a sensitivity study in which QuikSCAT wind

Table 2. Comparisons of QuikSCAT and in Situ 10 m Neutral Wind Speed After Correction of Possible in Situ Data Biases[a]

Region	Anemometer Type	$\langle U_{insitu} \rangle$ (m s^{-1})	σU_{insitu} (m s^{-1})	$\langle U_{qscat} \rangle$ (m s^{-1})	σU_{qscat} (m s^{-1})	$\frac{\langle U_{qscat} \rangle}{\langle U_{insitu} \rangle}$	$\frac{\langle U^2_{qscat} \rangle}{\langle U^2_{insitu} \rangle}$
North Atlantic	Debucourt cup	6.6	2.8	6.9	3.1	1.04	1.10
North Atlantic	Vector cup	8.5	3.3	8.8	3.7	1.04	1.08
Southern Ocean	Debucourt cup	8.7	2.9	9.1	3.2	1.05	1.12
Southern Ocean	Sonic	8.6	2.9	9.0	3.4	1.05	1.12

[a]CARIOCA-Debucourt wind speeds corrected for possible 8% underestimation, and in situ data acquired with Debucourt and Vector cup instruments corrected for 0.15 m s^{-1} bias possibly due to atmospheric stability effect.

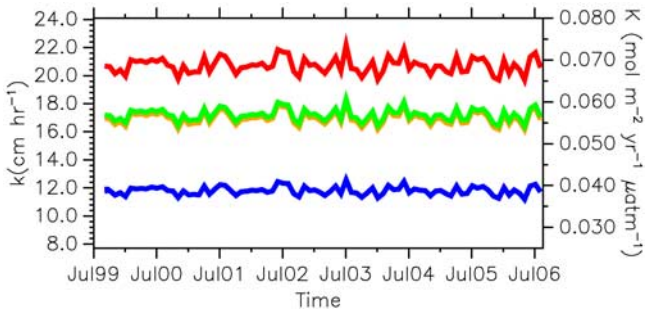

Figure 3. Monthly air-sea CO_2 transfer velocity k and exchange coefficient K deduced from QuikSCAT wind speeds from 1999 to 2006 using k-U relationships of *Liss and Merlivat* [1986] (blue), *Nightingale et al.* [2000] (green), *Ho et al.* [2006] (orange), and *Wanninkhof* [1992] (red) and integrated over the global ocean (80°S–80°N).

speeds are diminished by 5%, as a lower bound for the absolute accuracy of QuikSCAT wind speed.

4. Global k Average

4.1. QuikSCAT Estimate

[46] Averaged over 7 years, $\langle k_W \rangle$ and $\langle k_{LM} \rangle$ deduced from QuikSCAT wind speeds (21.1 and 11.9 cm h^{-1}, respectively (Figure 1)), differ by a ratio of 1.8. With respect to previous studies using older satellite wind speeds, they are higher by about 17% (Figure 1). When QuikSCAT wind speeds are lowered by 5%, $\langle k \rangle$ is lowered by 10% for a quadratic k-U relationship. Hence, the difference from previous satellite estimates becomes close to 6% (Figure 1). Nevertheless this difference remains larger than the interannual variability of k (see Figure 3 and Appendix B) and may be due to inaccuracies in previous satellite wind speeds. Indeed, *Boutin et al.* [1999b] show that the global k derived from ERS2 and NSCAT wind speeds differs by about 8%, partly because of ERS2 wind speed underestimation.

[47] The $\langle k_H \rangle$ (17.3 cm h^{-1}) and $\langle k_N \rangle$ (17.5 cm h^{-1}) differ by only 0.2 cm h^{-1} (1.2%) which is lower than the k-U relationships error estimate: *Ho et al.* [2006] estimate a precision of 0.019 (7%) in the coefficient of their quadratic relationship, which leads to a precision of 1.2 cm h^{-1} in the k global average. The $\langle k_N \rangle$ value is slightly higher than $\langle k_H \rangle$ although k_H is higher than k_N above 9 m s^{-1}, showing the importance of low to moderate wind speeds for the global k average, as already observed by *Boutin et al.* [2002]. The $\langle k_w \rangle$ differs from $\langle k_H \rangle$ and $\langle k_N \rangle$ by a ratio of 1.22 and 1.20, respectively.

4.2. Comparison With ^{14}C and Various Satellite Estimates of k

[48] The $\langle k \rangle$ values deduced from the new ^{14}C constraints, corrected with equation (7) when necessary, are reported on Figure 1. The three mean values estimated using the GEOSECS and the recent WOCE inventories by *Krakauer et al.* [2006], *Naegler et al.* [2006], and *Sweeney et al.* [2007] are consistent (within the error bars of each estimate). Nevertheless, we attach less confidence to the value reported by *Krakauer et al.* [2006], because it implies a linear dependency of k with wind speed, which is not observed in field data.

[49] The $\langle k \rangle$ values obtained with the *Liss and Merlivat* [1986] relationship and QuikSCAT wind speeds do not satisfy the new ^{14}C constraints proposed by *Krakauer et al.* [2006] and by *Naegler et al.* [2006] (Figure 1) and are in the lower bound of the estimate by *Sweeney et al.* [2007]. The $\langle k_H \rangle$ and $\langle k_N \rangle$ are in the upper part of the $\langle k \rangle$ estimates proposed by *Naegler et al.* [2006] and *Sweeney et al.* [2007]. Closer agreement is found with the new ^{14}C constraints proposed by *Naegler et al.* [2006] and *Sweeney et al.* [2007] with k_N derived from QuikSCAT wind speeds lowered by 5%. The 5% correction is not applied to k_H as the relationship presented by *Ho et al.* [2006] was deduced from QuikSCAT wind speeds. The $\langle k_W \rangle$ value derived from QuikSCAT wind speeds does not satisfy the new ^{14}C constraint of *Naegler et al.* [2006] and *Sweeney et al.* [2007]. When QuikSCAT wind speeds are lowered by 5%, $\langle k_w \rangle$ is in the upper error bar of these new ^{14}C estimates, but it remains 2.4 to 4.4 cm h^{-1} higher than their averages.

[50] It is interesting to compare $\langle k \rangle$ derived in this study with the one derived by *Frew et al.* [2007]. They used an empirical relationship between k and mean square slope (mss) based on field measurements and mss derived from dual frequency altimeter data, using a simple geometric optics model. They found a global mean k equal to 13.7 ± 4.1 cm h^{-1}, lower but consistent with our estimate of $\langle k_N \rangle$ and $\langle k_H \rangle$. Their mean estimate is closer to $\langle k_N \rangle$ after correcting QuikSCAT wind speed by 5%. This is consistent with the fact that the estimations of k during the CoOP97 campaign, used to calibrate k-mss relationship, were close to the *Nightingale et al.* [2000] k-U dependency [*Frew et al.*, 2004, Figure 4].

4.3. Consequences on Air-Sea CO_2 Flux

[51] Air-sea CO_2 fluxes are derived using equation (1) and ΔpCO_2 fields taken from the *Takahashi et al.* [2002] climatology. They are reported in Table 3 together with fluxes available at http://www.ldeo.columbia.edu/res/pi/CO2/carbondioxide/text/10m_wind.prn which were derived from the same ΔpCO_2 fields, the NCAR/NCEP 41-year reanalysis wind data at 10 m height [*Kistler et al.*, 2000], and the long-term *Wanninkhof* [1992] k-U relationship. The global flux we deduce from k_W and *Takahashi et al.* [2002] ΔpCO_2 fields is 8% more negative than that derived from 41 years of NCAR/NCEP reanalyzed wind speeds and the Wanninkhof long-term relationship (−1.64 Pg C a^{-1}). As shown by *Olsen et al.* [2005], this is mainly because of differences between NCAR/NCEP reanalysis wind speeds and QuikSCAT wind speeds. This is also partly consistent with the different variability between NCEP and QuikSCAT wind speed as seen by *Freilich and Vanhoff* [2006], which leads to a 4% difference in term of k (see section 3.1). All the fluxes indicated in Table 3 correspond to original QuikSCAT wind speeds. If QuikSCAT wind speeds are decreased by 5%, the absolute value of the fluxes would be decreased by 10% for quadratic relationships. With respect to the regional fluxes listed in Table 3, the greatest effect would be observed in the largest sink regions, between 14°S and 50°S.

Table 3. Net Sea-Air CO_2 Flux[a] With k-U Relationships[b]

Latitude Band	Wind Speed	K	Pacific	Atlantic	Indian	Southern	All Basins
North of 50°N	QuikSCAT	K_W	0.01	−0.35			−0.35
	QuikSCAT	K_H	0.01	−0.29			−0.30
	QuikSCAT	K_N	0.01	−0.29			−0.29
North of 50°N	NCEP	K_{WLT}	0.01	−0.31			−0.30
14°N–50°N	QuikSCAT	K_W	−0.54	−0.29	0.05		−0.77
	QuikSCAT	K_H	−0.44	−0.24	0.04		−0.63
	QuikSCAT	K_N	−0.44	−0.23	0.04		−0.63
14°N–50°N	NCEP	K_{WLT}	−0.50	−0.27			−0.72
14°S–14°N	QuikSCAT	K_W	0.74	0.13	0.17		1.04
	QuikSCAT	K_H	0.60	0.11	0.14		0.85
	QuikSCAT	K_N	0.64	0.11	0.14		0.90
14°S–14°N	NCEP	K_{WLT}	0.62	0.12	0.14		0.89
14°S–50°S	QuikSCAT	K_W	−0.37	−0.27	−0.63		−1.27
	QuikSCAT	K_H	−0.30	−0.22	−0.51		−1.04
	QuikSCAT	K_N	−0.30	−0.22	−0.52		−1.04
14°S–50°S	NCEP	K_{WLT}	−0.40	−0.24	−0.52		−1.16
South of 50°S	QuikSCAT	K_W				−0.41	−0.41
	QuikSCAT	K_H				−0.34	−0.34
	QuikSCAT	K_N				−0.34	−0.34
South of 50°S	NCEP	K_{WLT}				−0.35	−0.35
Total	QuikSCAT	K_W	−0.16	−0.78	−0.41	−0.41	−1.77
	QuikSCAT	K_H	−0.13	−0.64	−0.33	−0.34	−1.45
	QuikSCAT	K_N	−0.09	−0.63	−0.34	−0.34	−1.39
Total	NCEP	K_{WLT}	−0.27	−0.69	−0.33	−0.35	−1.64

[a]In Pg (10^{15} g) C a^{-1}. Deduced from *Takahashi et al.*'s [2002] ΔpCO_2 fields and QuikSCAT wind speeds between 1999 and 2006 (this study).
[b]From *Wanninkhof* [1992], *Ho et al.* [2006], and *Nightingale et al.* [2000]. For reference, fluxes available at http://www.ldeo.columbia.edu/res/pi/CO2/carbondioxide/text/10m_wind.prn and computed by Takahashi's group using *Takahashi et al.*'s [2002] ΔpCO_2 fields, NCAR/NCEP 41-year reanalysis wind data at 10 meter height [*Kistler et al.*, 2000], and the long-term *Wanninkhof* [1992] k-U relationship, K_{WLT}, are also reported.

[52] The global yearly air-sea CO_2 fluxes which we derive using k_w vary between −1.71 Pg C a^{-1} and −1.83 Pg C a^{-1} (7 years mean equal to −1.77 Pg C a^{-1}). These values are close to the 2000–2003 air-sea CO_2 fluxes derived by *Olsen et al.* [2005] using the same k-U relationship and QuikSCAT wind speeds (4 year mean equal to −1.73 Pg C a^{-1}). The variability of the fluxes in latitude obtained with k_w has already been discussed in previous studies [e.g., *Boutin et al.*, 2002; *Olsen et al.*, 2005]. In what follows, we concentrate on the differences linked to the use of different k-U relationships.

[53] If k_H, k_N or k_{LM} are used to compute the fluxes instead of k_W, the mean global absorbing flux is reduced to 1.45, 1.39 and 0.93 Pg C a^{-1}, respectively. The main differences in the regional fluxes are observed in regions where the fluxes are the greatest because of their large surface areas and/or because of the large disequilibrium between atmospheric and oceanic pCO_2, in the tropical band (decrease of the outgassing flux by 0.19 Pg C a^{-1} with k_H instead of k_W) and in the subtropics (decrease of the downward flux in the bands 14°N–50°N and 14°S–50°S by 0.37 Pg C a^{-1} when using k_H instead of k_W). Fluxes obtained with k_H and k_N are very similar except in the equatorial band because k_H is lower than k_N at low wind speed.

[54] The mean global absorbing fluxes deduced from k_H and k_N are 1.45 and 1.39 Pg C a^{-1}, respectively. However, uncertainty remains in these estimates: given the absolute accuracy in QuikSCAT wind speed and in the new ^{14}C constraint, the flux may be overestimated by 10% at most. In addition, ΔpCO_2 fields are going to be reduced in future estimates as *Takahashi et al.* [2002] did not correct ocean pCO_2 measurements for the atmospheric trend in some regions, although recent studies have shown that a correction should be applied [*Feely et al.*, 2006; *Rangama et al.*, 2005]. This correction should lead to a significant decrease in absorbing air-sea CO_2 flux (see T. Takahashi et al., Improved estimates for the climatological mean distribution of sea-air pCO_2 difference and the net CO_2 flux over the global oceans, paper presented at Ocean Carbon Biogeochemistry Workshop, Woods Hole Oceanographic Institution, Woods Hole, Massachusetts, 2006).

5. Summary and Conclusions

[55] The quality of satellite wind speeds has greatly improved over the last two decades, and today estimates of the root mean squared accuracies of scatterometer wind speeds are around 1 m s^{-1}. This makes it possible to monitor wind speed variability very well. Nevertheless, when dealing with parameters proportional to the square of U, such as k, the absolute accuracy requirement for both mean and standard deviation of wind speed is very stringent. Given previous QuikSCAT wind speed validation studies and the new comparisons shown in this paper, we conclude that the QuikSCAT operational products are accurate to 5% or better. The new comparisons demonstrate the difficulty of assessing the absolute accuracy of satellite wind speeds over the global ocean, given the difficulty of acquiring high-quality estimates of neutral equivalent wind speed over various regions of the open ocean and they provide QuikSCAT-buoy wind speed comparisons in the Southern Ocean for the first time. Buoy wind speed data used for satellite wind speed validation have typically been acquired at a height lower than 10 m, in nonneutral conditions and in the tropics or in the northern hemisphere. In our $\langle k \rangle$ determinations, QuikSCAT operational products are used as the reference wind speed; however, given the results

Table A1. Colocation Periods of QuikSCAT With in Situ Wind Speed

Period of Wind Measurements	Buoy Type	Ocean Sector	Anemometer Type
9 Feb 2001 to 31 Dec 2001	CARIOCA	North Atlantic	Debucourt cup
27 Aug 2000 to 3 May 2001	Moored buoy	North Atlantic	Vector cup
20 Nov 2001 to 29 Dec 2001	CARIOCA	Southern Ocean	Debucourt cup
13 Jan 2002 to 3 Mar 2002	CARIOCA	Southern Ocean	Debucourt cup
13 Jan 2002 to 13 Mar 2002	CARIOCA	Southern Ocean	Debucourt cup
30 Jan 2003 to 22 Apr 2003	CARIOCA	Southern Ocean	Debucourt cup
31 Jan 2006 to 10 Jul 2006	CARIOCA	Southern Ocean	Sonic

of our new comparisons, we have also performed a sensitivity study in which QuikSCAT wind speeds are diminished by 5%, making the implicit assumption that the actual neutral wind speed is bounded between the QuikSCAT value and the QuikSCAT value minus 5%.

[56] The $\langle k_H \rangle$ and $\langle k_N \rangle$ differ by 1.5% when QuikSCAT wind speeds are used for their computation. The polynomial function used by *Nightingale et al.* [2000] was chosen because the *Liss and Merlivat* [1986] relationship, which is physically based, fitted better with a second-order polynomial function than with a quadratic function. However, the differences we observe are within the precision of these relationships. The $\langle k_{LM} \rangle$ and $\langle k_W \rangle$ are quite far from new ^{14}C derived $\langle k \rangle$ although, given the uncertainty of QuikSCAT wind speeds and on ^{14}C k estimates, they remain at the very lower and very upper bounds of the error intervals (Figure 1). On the other hand, the $\langle k_H \rangle$ and $\langle k_N \rangle$ are fully consistent with new ^{14}C constraints. Hence, the introduction of an ''inventory normalized gas exchange parameter'' intended to adjust $\langle k \rangle$ to ^{14}C constraint for a given wind field, as proposed by *Naegler et al.* [2006], is not relevant when using high-resolution QuikSCAT wind speed. Indeed, the difference between QuikSCAT $\langle k \rangle$ and ^{14}C constraint may either be due to a bias in QuikSCAT wind speeds or to uncertainties in ^{14}C values. On the other hand, if QuikSCAT wind speeds are overestimated by 5%, the coefficient of the k-U relationships determined by *Ho et al.* [2006] should be increased by 10% (as the relationship was derived using QuikSCAT wind speeds).

[57] Taking into account wind speed uncertainty, the global mean of air-sea CO_2 fluxes derived with the transfer velocities that are in close agreement with new ^{14}C constraints (k_H and k_N) and with ΔpCO_2 fields taken from *Takahashi et al.*'s [2002] climatology, is between -1.36 and -1.45 Pg C a^{-1}. Although the calibration of k-U relationships has been greatly advanced by the new ^{14}C inventories, new experiments are still needed (1) to analyze the impact of sea surface parameters other than U on k, (2) to study the impact of such alternative parameterizations on global k fields with respect to k-scatterometer U fields, and (3) to improve the k-U relationships by additional in situ flux measurements. It is critical to measure wind speeds very accurately, as a 5% bias in U leads to a 10% bias in k.

Appendix A: In Situ Wind Speed Colocated With QuikSCAT Wind Speeds

[58] Periods and locations of QuikSCAT in situ wind speeds colocations are summarized in Table A1. In the northern Atlantic, CARIOCA drifters were deployed and drifted between 36°N and 46°N and 12°W and 22°W; trajectories are presented by *Merlivat et al.* [2009]. In the Southern Ocean, they drifted in the southern Atlantic ocean and in the Indian Ocean as shown in Figure A1.

Appendix B: Air-Sea CO_2 Exchange Coefficients

[59] For each 25 km resolution QuikSCAT wind speed, k is computed using relationships (2) through (5). These relationships are restated in Figure B1.

[60] The temperature–Schmidt number dependency is taken from *Wanninkhof* [1992]. An estimate of K is obtained by multiplying k by the solubility derived using the temperature-solubility dependence given by *Weiss* [1974]. K deduced with the k-U relationships of *Liss and Merlivat* [1986], *Wanninkhof* [1992], *Nightingale et al.*

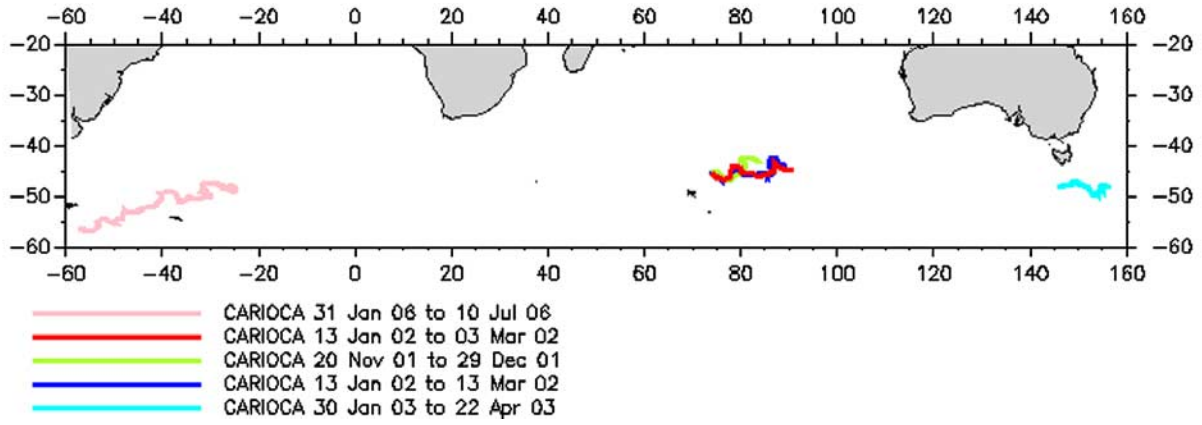

Figure A1. CARIOCA wind speeds location in the Southern Ocean.

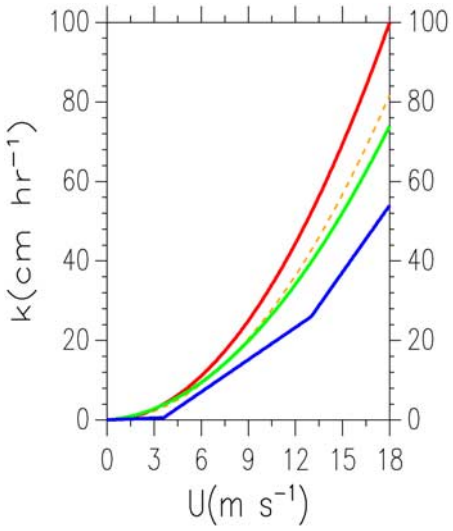

Figure B1. The k-U relationships at 20°C (Sc = 660) from *Liss and Merlivat* [1986] (blue), *Nightingale et al.* [2000] (green), *Ho et al.* [2006] (orange), and *Wanninkhof* [1992] (red).

[2000], and *Ho et al.* [2006] are named K_{LM}, K_W, K_N and K_H, respectively.

[61] Weekly and monthly 1° × 1° resolution K maps are obtained by interpolating K using the IFREMER kriging method described by *Bentamy et al.* [1996]. This method was validated by the comparison of satellite interpolated wind speeds with in situ wind speeds and it is routinely used at CERSAT/IFREMER for wind speed interpolations *Bentamy and Piollé* [2002]. In order to ensure consistency with previous K fields derived using a simpler objective analysis method [*Boutin and Etcheto*, 1997], at LODYC (Laboratoire d'Océanographie Dynamique et de Climatologie), K maps obtained with the two methods were compared.

[62] The K global average deduced from QuikSCAT wind speeds with the IFREMER interpolation method over 5 years is only 0.7% higher than the K global average deduced from the LODYC method. This result was obtained with the nonlinear *Liss and Merlivat* [1986] and the *Wanninkhof* [1992] quadratic relationships. The standard deviation of the differences between LODYC and IFREMER K_{LM} interpolated on weekly fields at 1° × 1° resolution is 0.38 × 10^{-2} mol m^{-2} a^{-1} μatm^{-1}, i.e., 10% of the global K

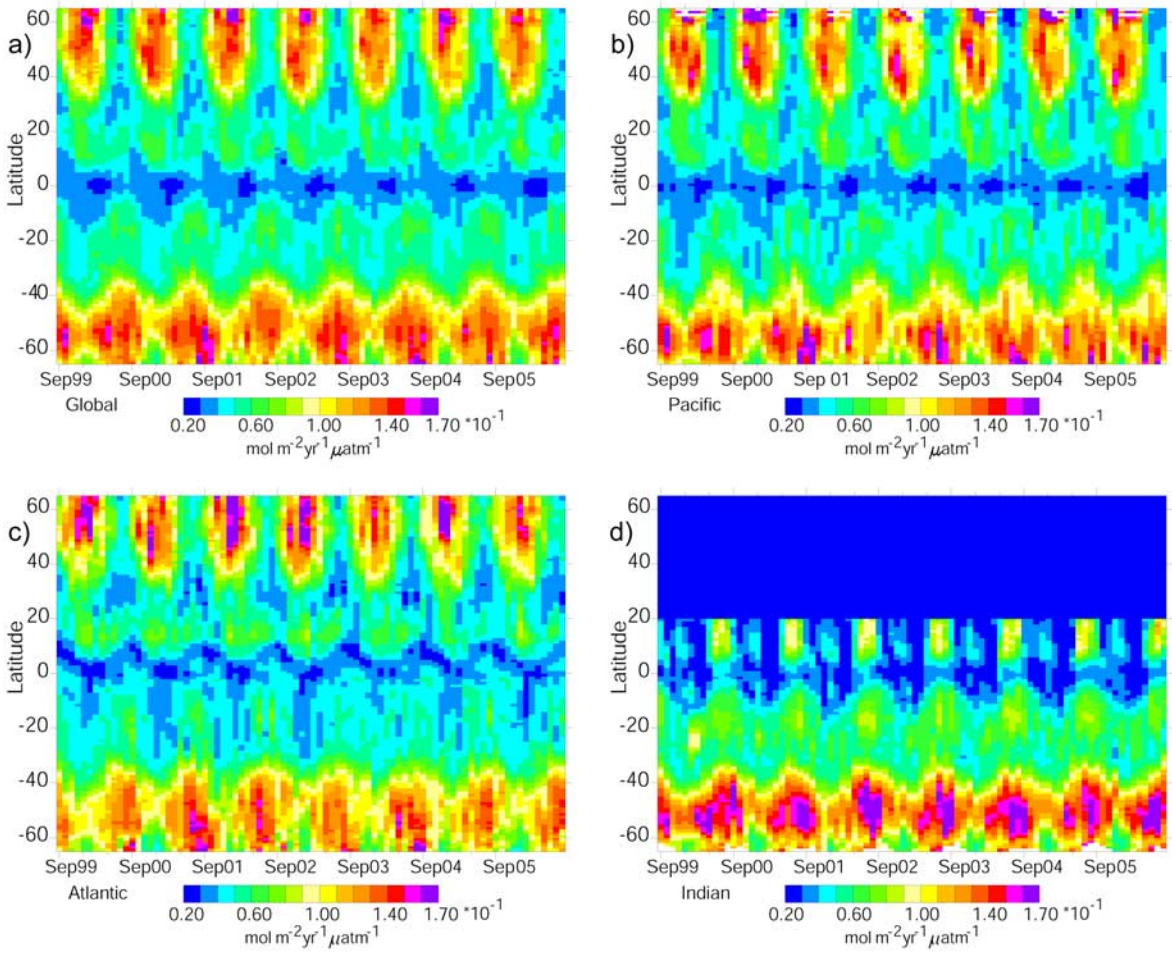

Figure B2. Monthly zonal average of K_W from September 1999 to September 2006 derived from QuikSCAT wind speeds. (a) Global ocean, (b) Pacific Ocean, (c) Atlantic Ocean, and (d) Indian Ocean. The same patterns would be obtained for K derived with the *Ho et al.* [2006] k-U relationship with a color scale ranging from 0.02 to 0.14 mol m^{-2} a^{-1} μatm^{-1} (1 atm = 10^5 × 1.01325 N m^{-2}); this corresponds to approximately 5 cm h^{-1} to 46 cm h^{-1} for k_{H660} (see text).

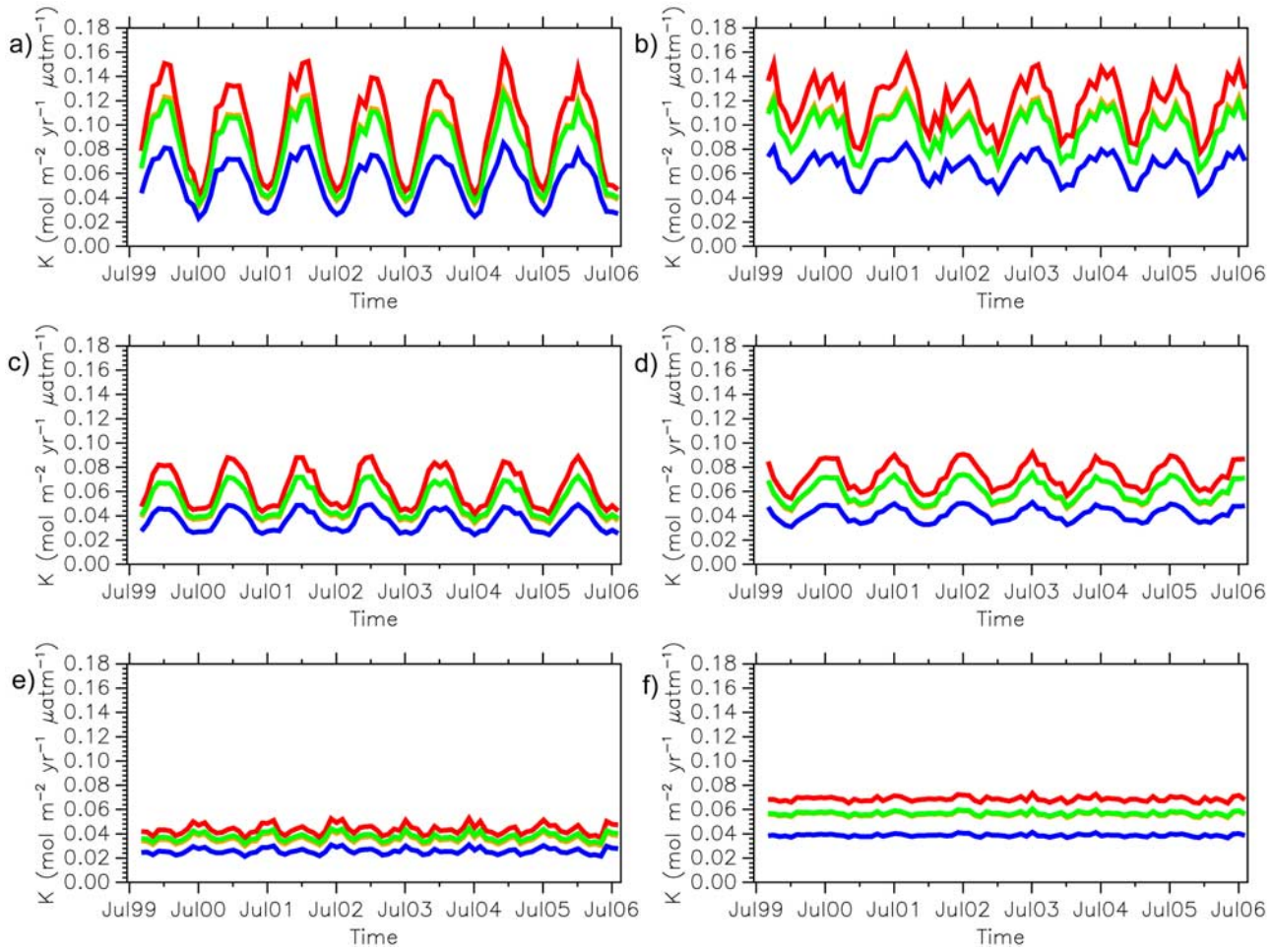

Figure B3. Monthly CO_2 exchange coefficients deduced from QuikSCAT wind speeds and k-U relationships of *Liss and Merlivat* [1986] (blue), *Nightingale et al.* [2000] (green), *Ho et al.* [2006] (orange), and *Wanninkhof* [1992] (red) and integrated over latitudinal bands. High latitude at (a) 50°N–80°N and (b) 50°S–80°S, midlatitudes at (c) 14°N–50°N and (d) 14°S–50°S, (e) tropics at 14°S–14°N, and (f) global ocean at 80°N–80°S.

average. This is mainly because the LODYC method smoothes more small scale spatial variations than the IFREMER method.

[63] Monthly zonal averages of K derived with the *Wanninkhof* [1992] k-U relationship are presented in Figure B2. This k-U relationship was chosen because it is the most widely used in the scientific community. Figure B2 results can be converted to other quadratic k-U relationships ($k = aU^2 (660/Sc)^{0.5}$) by multiplying the color scale by a/0.31. So, for the *Ho et al.* [2006] relationship, the scale has to be multiplied by 0.818 and ranges from 0.017 to 0.15 mol m^{-2} a^{-1} μatm^{-1}.

[64] Monthly zonal averages of K follow the classical latitudinal and seasonal variations [*Boutin and Etcheto*, 1997]: minimum of K in the tropics, maximum at high latitudes with a seasonal cycle much weaker in the Southern Ocean than at high northern latitudes, K stronger in the southern Indian Ocean than in the southern Pacific and Atlantic Ocean. In addition, monthly K averaged over all longitudes exhibits interannual variability, e.g., a decrease of K in the Southern Ocean during the austral winter 2002 due to K decrease in the southern Pacific Ocean, a decrease of K in boreal winters 2003–2004 and 2005–2006 in the high northern latitudes due to K decrease in the Atlantic Ocean, and an increase of K at the end of 2003 in the southern tropics.

[65] The mean monthly K values obtained with the four k-U relationships in five latitudinal bands and over the global ocean are shown in Figure B3. For all latitudinal band, K_{LM} is lower than K_N which in turn is lower than K_W. The ratios between the various K are variable depending on the wind speed distribution in the latitudinal band, as already discussed by *Boutin et al.* [2002]. K_N and K_H are very close to each other as is to be expected from the k-U relationships (see Figure A1): both k-U relationships give the same k at 7.6 m s^{-1}. For lower U, k_N is slightly higher than k_H (a difference of less than 1 cm h^{-1}) and for higher U, k_N is lower than k_H. The difference remains less than 10% for U up to 16 m s^{-1}. These small differences lead to a peak-to-peak seasonal variation of K that is about 5% higher for K_H than for K_N in the high northern latitudes (Figure B3a). When averaged over the global ocean, K exhibits no seasonal variation. Mean global values (and the standard deviation of monthly mean global values from September

1999 to August 2006) of K_W, K_H, K_N and K_{LM} are 6.86 (±0.18), 5.61 (±0.15), 5.69 (±0.14), and 3.88 (±0.10) × 10^{-2} mol m^{-2} a^{-1} μatm^{-1}, respectively.

[66] Using the conversion factors given in section 2.2.1, the color scale of Figure B2 corresponds approximately to k_H at a Schmidt number of 660 varying from 5 cm h^{-1} to 46 cm h^{-1}. The seasonal and interannual variability seen on monthly zonal k distributions derived from our Figure B2 are very similar to the ones derived from the altimetric mss and k-mss relationship by *Glover et al.* [2007] as shown on their Figure 4. In particular, both studies show a decrease of k in the Southern Ocean during the austral winter 2002, a decrease of k in the boreal winter 2003–2004 in the high northern latitudes and an increase of k at the end of 2003 in the southern tropics.

[67] **Acknowledgments.** We thank three anonymous reviewers for constructive remarks. This study was supported by a research agreement between the IFREMER and LODYC institutes and by the FP6 CarboOcean European project. We are indebted to N. Martin for data processing and software development and to O. Coze for handling comparisons of LODYC and IFREMER K grids. We thank T. Takahashi for providing his pCO_2 climatology and for fruitful discussions about oceanic pCO_2 trends. We thank S. Arnault for helpful discussions about altimetry. QuikSCAT K fields are routinely processed and are available on the CERSAT/IFREMER ftp site ftp.ifremer.fr (directory/ifremer/cersat/products/gridded/kco2-quikscat/). Software for reading and colocating K maps with in situ data is available at http://www.locean-ipsl.upmc.fr/index.php?option=com_content&task=view&id=44&Itemid=64.

References

Bakker, D. C. E., J. Etcheto, J. Boutin, and L. Merlivat (2001), Variability of surface-water fCO_2 during seasonal upwelling in the equatorial Atlantic Ocean as observed by a drifting buoy, *J. Geophys. Res.*, *106*, 9241–9254, doi:10.1029/1999JC000275.

Bentamy, A., and J. F. Piollé (2002), QuikSCAT scatterometer mean wind fields product — User manual, *Rep. C2-MUT-W-03-IF*, Inst. Fr. de Rech. pour l'Exploit. de la Mar, Brest, France.

Bentamy, A., Y. Quilfen, F. Gohin, N. Grima, M. Lenaour, and J. Servain (1996), Determination and validation of average wind fields from ERS-1 scatterometer measurements, *Global Atmos. Ocean Syst.*, *4*, 1–29.

Bourassa, M. A., D. M. Legler, J. J. O'Brien, and S. R. Smith (2003), SeaWinds validation with research vessels, *J. Geophys. Res.*, *108*(C2), 3019, doi:10.1029/2001JC001028.

Boutin, J., and J. Etcheto (1996), Consistency of Geosat, SSM/I and ERS1 global surface wind speeds — Comparison with in situ data, *J. Atmos. Oceanic Technol.*, *13*, 183–197, doi:10.1175/1520-0426(1996)013<0183:COGSAG>2.0.CO;2.

Boutin, J., and J. Etcheto (1997), Long term variability of the air-sea CO_2 exchange coefficient: Consequences for the CO_2 fluxes in the equatorial Pacific Ocean, *Global Biogeochem. Cycles*, *11*, 453–470, doi:10.1029/97GB01367.

Boutin, J., et al. (1999a), Satellite sea surface temperature: A powerful tool for interpreting in situ pCO_2 measurements in the equatorial Pacific Ocean, *Tellus, Ser. B*, *51*, 490–508, doi:10.1034/j.1600-0889.1999.00025.x.

Boutin, J., J. Etcheto, M. Rafizadeh, and D. C. E. Bakker (1999b), Comparison of NSCAT, ERS 2 active microwave instrument, special sensor microwave imager, and Carbon Interface Ocean Atmosphere buoy wind speed: Consequences for the air-sea CO_2 exchange coefficient, *J. Geophys. Res.*, *104*, 11,375–11,392, doi:10.1029/1998JC900119.

Boutin, J., J. Etcheto, L. Merlivat, and Y. Rangama (2002), Influence of gas exchange coefficient parameterization on seasonal and regional variability of CO_2 air-sea fluxes, *Geophys. Res. Lett.*, *29*(8), 1182, doi:10.1029/2001GL013872.

Boutin, J., L. Merlivat, C. Hénocq, N. Martin, and J. B. Sallée (2008), Air-sea CO_2 flux variability in frontal regions of the Southern Ocean from CARIOCA drifters, *Limnol. Oceanogr.*, *53*, 2062–2079.

Caniaux, G., A. Brut, D. Bourras, H. Giordani, A. Paci, L. Prieur, and G. Reverdin (2005), A 1 year sea surface heat budget in the northeastern Atlantic basin during the POMME experiment: 1. Flux estimates, *J. Geophys. Res.*, *110*, C07S02, doi:10.1029/2004JC002596.

Carr, M.-E., W. Tang, and W. T. Liu (2002), CO_2 exchange coefficients from remotely sensed wind speed measurements: SSM/I versus QuikSCAT in 2000, *Geophys. Res. Lett.*, *29*(15), 1740, doi:10.1029/2002GL015068.

Drennan, W. M., P. K. Taylor, and M. J. Yelland (2005), Parameterizing the sea surface roughness, *J. Phys. Oceanogr.*, *35*, 835–848, doi:10.1175/JPO2704.1.

Ebuchi, N., H. C. Graber, and M. J. Caruso (2002), Evaluation of wind vectors observed by QuikSCAT/SeaWinds using ocean buoy data, *J. Atmos. Oceanic Technol.*, *19*, 2049–2062, doi:10.1175/1520-0426(2002)019<2049:EOWVOB>2.0.CO;2.

Etcheto, J., and L. Merlivat (1988), Satellite determination of the carbon dioxide exchange coefficient at the ocean-atmosphere interface: A first step, *J. Geophys. Res.*, *93*, 15,669–15,678, doi:10.1029/JC093iC12p15669.

Etcheto, J., J. Boutin, Y. Dandonneau, D. C. E. Bakker, R. A. Feely, R. D. Ling, P. D. Nightingale, and R. Wanninkhof (1999), Air-sea CO_2 flux variability in the equatorial Pacific Ocean east of 100°W, *Tellus, Ser. B*, *51*, 734–747, doi:10.1034/j.1600-0889.1999.t01-1-00013.x.

Feely, R. A., et al. (2002), Seasonal and interannual variability of CO_2 in the equatorial Pacific, *Deep Sea Res., Part II*, *49*, 2443–2469, doi:10.1016/S0967-0645(02)00044-9.

Feely, R. A., T. Takahashi, R. Wanninkhof, M. J. McPhaden, C. E. Cosca, S. C. Sutherland, and M. Carr (2006), Decadal variability of the air-sea CO_2 fluxes in the equatorial Pacific Ocean, *J. Geophys. Res.*, *111*, C08S90, doi:10.1029/2005JC003129.

Freilich, M. H., and B. A. Vanhoff (2006), The accuracy of preliminary Windsat vector wind measurements: Comparison with NDBC buoys and QuikSCAT, *IEEE Trans. Geosci. Remote Sens.*, *44*, 622–637, doi:10.1109/TGRS.2006.869928.

Frew, N. M., et al. (2004), Air-sea gas transfer: Its dependence on wind stress, small-scale roughness and surface films, *J. Geophys. Res.*, *109*, C08S17, doi:10.1029/2003JC002131.

Frew, N. M., D. M. Glover, E. J. Bock, and S. J. McCue (2007), A new approach to estimation of global air-sea gas transfer velocity fields using dual-frequency altimeter backscatter, *J. Geophys. Res.*, *112*, C11003, doi:10.1029/2006JC003819.

Glover, D. M., N. M. Frew, and S. J. McCue (2007), Air-sea gas transfer velocity estimates from the Jason-1 and TOPEX altimeters: Prospects for a long-term global time series, *J. Mar. Syst.*, *66*, 173–181, doi:10.1016/j.jmarsys.2006.03.020.

Ho, D. T., C. S. Law, M. J. Smith, P. Schlosser, M. Harvey, and P. Hill (2006), Measurements of air-sea gas exchange at high wind speeds in the Southern Ocean: Implications for global parameterizations, *Geophys. Res. Lett.*, *33*, L16611, doi:10.1029/2006GL026817.

Hood, E. M., and L. Merlivat (2001), Annual to interannual variations of fCO_2 in the northwestern Mediterranean Sea: High frequency time series data from CARIOCA buoys (1995–1997), *J. Mar. Res.*, *59*, 113–131, doi:10.1357/002224001321237399.

Kara, A. B., E. J. Metzger, and M. A. Bourassa (2007), Ocean current and wave effects on wind stress drag coefficient over the global ocean, *Geophys. Res. Lett.*, *34*, L01604, doi:10.1029/2006GL027849.

Kelly, K. A., S. Dickinson, M. J. McPhaden, and G. C. Johnson (2001), Ocean currents evident in satellite wind data, *Geophys. Res. Lett.*, *28*, 2469–2472, doi:10.1029/2000GL012610.

Key, R. M., A. Kozyr, C. L. Sabine, K. Lee, R. Wanninkhof, J. L. Bullister, R. A. Feely, J. F. Millero, C. Mordy, and T. H. Peng (2004), A global ocean carbon climatology: Results from Gobal Data Analysis Project (GLODAP), *Global Biogeochem. Cycles*, *18*, GB4031, doi:10.1029/2004GB002247.

Kistler, R., et al. (2000), The NCEP–NCAR 50-Year Reanalysis: Monthly Means CD-ROM and Documentation, *Bull. Am. Geophys. Soc.*, *82*, 247–267.

Krakauer, N. Y., J. T. Randerson, F. W. Primeau, N. Gruber, and D. Menemenlis (2006), Carbon isotope evidence for the latitudinal distribution and wind speed dependence of the air-sea transfer velocity, *Tellus, Ser. B*, *58*, 390–417.

Lefèvre, N., J. Aiken, J. Rutllant, G. Daneri, S. Lavender, and T. Smyth (2002), Observations of pCO_2 in the coastal upwelling off Chile: Spatial and temporal extrapolation using satellite data, *J. Geophys. Res.*, *107*(C6), 3055, doi:10.1029/2000JC000395.

Liss, P. S., and L. Merlivat (1986), Air-sea gas exchange rates: Introduction and synthesis, in *The Role of Air-Sea Exchange in Geochemical Cycling*, edited by P. Buat-Ménart, pp. 113–127, D. Reidel, Norwell, Mass.

Liu, W. T., and W. Tang (1996), Equivalent neutral wind, report, 8 pp., Jet Propul. Lab, Pasadena, Calif.

Merlivat, L., and P. Brault (1995), CARIOCA buoy: Carbon dioxide monitor, *Sea Technol.*, *10*, 23–30.

Merlivat, L., M. G. Davila, G. Caniaux, J. Boutin, and G. Reverdin (2009), Mesoscale and diel to monthly variability of CO_2 and carbon fluxes at the ocean surface in the northeastern Atlantic, *J. Geophys. Res.*, *114*, C03010, doi:10.1029/2007JC004657.

Naegler, T., and I. Levin (2006), Closing the global radiocarbon budget 1945–2005, *J. Geophys. Res.*, *111*, D12311, doi:10.1029/2005JD006758.

Naegler, T., P. Ciais, K. B. Rodgers, and I. Levin (2006), Excess radiocarbon constraints on air-sea gas exchange and the uptake of CO_2 by the oceans, *Geophys. Res. Lett.*, *33*, L11802, doi:10.1029/2005GL025408.

Nightingale, P. D., G. Malin, C. S. Law, A. J. Watson, P. S. Liss, M. I. Liddicoat, J. Boutin, and R. C. Upstill-Goddard (2000), In-situ evaluation of air-sea gas exchange parameterizations using novel conservative and volatile tracers, *Global Biogeochem. Cycles*, *14*, 373–387, doi:10.1029/1999GB900091.

Olsen, A., R. Waninkhof, J. A. Trinanes, and T. Johannessen (2005), The effect of wind speed products and wind speed–gas exchange relationships on interannual variability of the air-sea CO_2 gas transfer velocity, *Tellus, Ser. B*, *57*, 95–106, doi:10.1111/j.1600-0889.2005.00134.x.

Peacock, S. (2004), Debate over the ocean bomb radiocarbon sink: Closing the gap, *Global Biogeochem. Cycles*, *18*, GB2022, doi:10.1029/2003GB002211.

Queffeulou, P., S. Didailler, R. Ezraty, A. Bentamy, and J. P. Gouillou (1988), Toscane 2 campaign report, report, Inst. Fr. de Rech. pour l'Exploit. de la Mar, Brest, France.

Quilfen, Y., B. Chapron, and V. Vandemark (2001), The ERS scatterometer wind measurement accuracy: Evidence of seasonal and regional biases, *J. Atmos. Oceanic Technol.*, *18*, 1684–1697, doi:10.1175/1520-0426(2001)018<1684:TESWMA>2.0.CO;2.

Quilfen, Y., C. Prigent, B. Chapron, A. A. Mouche, and N. Houtin (2007), The potential of QuikSCAT and WindSat observations for the estimations of sea surface wind vector under severe weather conditions, *J. Geophys. Res.*, *112*, C09023, doi:10.1029/2007JC004163.

Rangama, Y., J. Boutin, J. Etcheto, L. Merlivat, T. Takahashi, B. Delille, M. Frankignoulle, and D. C. E. Bakker (2005), Variability of the net air–sea CO_2 flux inferred from shipboard and satellite measurements in the Southern Ocean south of Tasmania and New Zealand, *J. Geophys. Res.*, *110*, C09005, doi:10.1029/2004JC002619.

Reynolds, R. W., N. A. Rayner, T. M. Smith, D. C. Stokes, and W. Wang (2002), An improved in situ and satellite SST analysis for climate, *J. Clim.*, *15*, 1609–1625, doi:10.1175/1520-0442(2002)015<1609:AIISAS>2.0.CO;2.

Sabine, C. L., et al. (2004), The oceanic sink for anthropogenic CO_2, *Science*, *305*, 367–371, doi:10.1126/science.1097403.

Sweeney, C., E. Gloor, A. R. Jacobson, R. M. Key, G. McKinley, J. L. Sarmiento, and R. Wanninkhof (2007), Constraining global air-sea gas exchange for CO_2 with recent bomb ^{14}C measurements, *Global Biogeochem. Cycles*, *21*, GB2015, doi:10.1029/2006GB002784.

Takahashi, T., et al. (2002), Global sea-air CO_2 flux based on climatological surface ocean pCO_2 and seasonal biological and temperature effects, *Deep Sea Res., Part II*, *49*, 1601–1622, doi:10.1016/S0967-0645(02)00003-6.

Wanninkhof, R. (1992), Relationship between wind speed and gas exchange over the ocean, *J. Geophys. Res.*, *97*, 7373–7382, doi:10.1029/92JC00188.

Wanninkhof, R. (2007), The impact of different gas exchange formulations and wind speed products on global air-sea CO_2 fluxes, in *Transport at The Air Sea Interface*, edited by C. S. Garbe, R. A. Handler, and B. Jähne, pp. 1–23, Springer, Berlin.

Wanninkhof, R., S. C. Doney, T. Takahashi, and W. R. McGillis (2002), The effect of using time-averaged winds on regional air-sea CO_2 fluxes, in *Gas Transfer at Water Surfaces, Geophys. Monogr. Ser.*, vol. 127, edited by M. A. Donelan et al., pp. 351–356, AGU, Washington, D. C.

Weiss, R. F. (1974), Carbon dioxide in water and seawater: The solubility of a nonideal gas, *Mar. Chem.*, *2*, 203–215, doi:10.1016/0304-4203(74)90015-2.

J. Boutin and L. Merlivat, Laboratoire d'Océanographie et du Climat, UMR7159, UPMC, Expérimentation et Approches Numériques, Institut Pierre Simon Laplace, CNRS, F-75252 Paris, France. (jb@locean-ipsl.upmc.fr)

J. F. Piolle and Y. Quilfen, Laboratoire d'Océanographie Spatiale, IFREMER, F-29280 Brest, France.